

Neural Activity in Primate Parietal Area 7a Related to Spatial Analysis of Visual Mazes

David A. Crowe^{1,2}, Matthew V. Chafee^{1,3},
Bruno B. Averbeck^{1,2} and Apostolos P. Georgopoulos¹⁻⁵

¹Brain Sciences Center, Veterans Affairs Medical Center, Minneapolis, MN, ²Graduate Program in Neuroscience, University of Minnesota, Minneapolis, MN, Departments of ³Neuroscience, ⁴Neurology and ⁵Psychiatry, University of Minnesota Medical School, Minneapolis, MN, USA

Cognitive psychological studies of humans and monkeys solving visual mazes have provided evidence that a covert analysis of the maze takes place during periods of eye fixation interspersed between saccades, or when mazes are solved without eye movements. We investigated the neural basis of this process in posterior parietal cortex by recording the activity of single neurons in area 7a during maze solution. Monkeys were required to determine from a single point of fixation whether a critical path through the maze reached an exit or a blind ending. We found that during this process the activity of approximately one in four neurons in area 7a was spatially tuned to maze path direction. We obtained evidence that path tuning did not reflect a covert saccade plan insofar as the majority of neurons active during maze solution were not active on a delayed-saccade control task, and the minority that were active on both tasks did not exhibit congruent spatial tuning in the two conditions. We also obtained evidence that path tuning during maze solution was not due to the locations of visual receptive fields mapped outside the behavioral context of maze solution, in that receptive field centers and preferred path directions were not spatially aligned. Finally, neurons tuned to path direction were not present in area 7a when a naïve animal viewed the same visual maze stimuli but did not solve them. These data support the hypothesis that path tuning in parietal cortex is not due to the lower level visual features of the maze stimulus, but rather is associated with maze solution, and as such, reflects a cognitive process applied to a complex visual stimulus.

Keywords: area 7a, directional tuning, monkey, parietal cortex, spatial cognition

Introduction

In previous psychophysical studies of human performance during the solution of visual mazes, we found that subjects made a sequence of saccades forming a scan path that accurately followed the underlying maze path that the subjects processed (Crowe *et al.*, 2000). The fact that the endpoint of each saccade accurately targeted the followed maze path indicated a prior neural representation of the course of the path through the visual periphery. Here we investigate this neural representation in parietal area 7a of macaques trained to solve visual mazes without making eye movements.

In prior studies, it was found that the analysis of maze structure was a time consuming process independent of oculomotor output. For example, fixation time between saccades depended on the length and complexity of maze path intervening between the current point of fixation and the next (Crowe *et al.*, 2000). The same relation held when either monkeys or humans solved visual mazes from a single point of fixation (Chafee *et al.*, 2002). Our working theory of this

spatial process is that a spatial representation of the forthcoming section of the path is generated while the eyes remain fixed in position. The analysis is directional, and operates over a limited spatial extent. Once the analysis of the maze path has reached this limit, the endpoint of the next saccade is determined, resetting the process. In essence, the hypothesis is that the mind leads through the maze, and the eyes catch up.

Here we report that neural activity in area 7a is spatially tuned to the direction of a processed maze path in the absence of eye movements. Evidence from control experiments argued against the possibility that this neural signal reflected oculomotor intention. Further, path tuning functions during maze solution were not aligned to visual receptive fields mapped outside the context of maze solution. Our data support the hypothesis that the path tuning of area 7a neurons reflects their participation in a goal-driven spatial analysis of visual maze stimuli.

Materials and Methods

Subjects

Two monkeys, κκ and ππ (*Macaca mulatta*, 5–7 kg body wt) were trained to solve visual mazes while maintaining eye fixation at the center of the display. An additional monkey, ττ (*M. mulatta*, 4.5 kg) was trained in a passive fixation task, in which mazes were shown but were not solved. Care and treatment of the animal conformed to the Principles of Laboratory Animal Care of the NIH (NIH publication no. 86-23, revised in 1995). The Internal Animal Care and Use Committees of the University of Minnesota and the Minneapolis Veterans Affairs Medical Center approved all experimental protocols.

Tasks

A trial began when the monkeys' eye position was within 1.5° of visual angle (DVA) from a central fixation target. Eye position was monitored using the scleral search coil technique in monkey κκ (Fuchs and Robinson, 1966) (CNC Engineering, Seattle, WA), and an infrared eye tracking system in the others (ISCAN, Burlington, MA). The horizontal and vertical components of the eye position were recorded at a sampling rate of 200 Hz (eye coil) or 60 Hz (infrared eye tracking system) simultaneously with neural recordings. After a variable interval of 600–840 ms, an octagonal maze (Fig. 1) was displayed on a liquid crystal display projection screen at eye level directly in front of the monkey. The maze was composed of white lines (separated by 2.7 DVA) on a black background and subtended 30 × 30 DVA. It contained a central start box and a straight path extending outwards from the start box in one of eight radial directions. This path either extended to the perimeter of the maze (exit maze, Fig. 1, left) or terminated one path width (2.7 DVA) from the perimeter of the maze (no-exit maze, Fig. 1, right). Maze fragments in the remaining interior area of the maze were randomly generated. Since there was a gap in the perimeter of the maze for an exit path, two more such gaps (for a total of three) were added at random locations in the perimeter to ensure that the monkeys could not solve the maze based on the presence of a gap. In the case of a no-exit maze, three gaps were randomly added to the maze perimeter to keep the number of gaps constant across exit and no-exit mazes. After

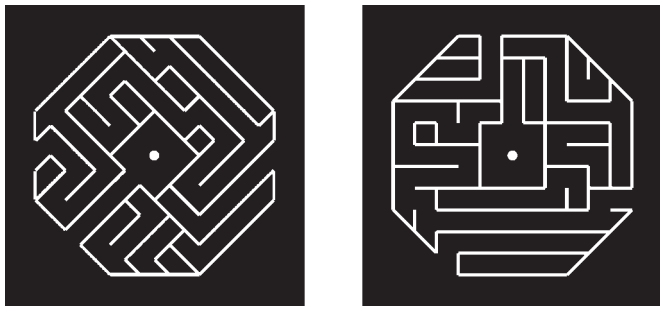


Figure 1. Examples of maze stimuli. All maze stimuli were centered on the fixation dot at the center of the display. Each maze contained a 'start box' (square region at the center of the maze surrounding the fixation dot), and a 'main path', which was the single, straight maze path that was continuous with the start box. In the maze on the left, the main path is oriented down and to the left. In the maze on the right, the main path is oriented straight up. Maze stimuli were of two types. Exit mazes were those in which the main path led continuously from the start box to an exit in the maze perimeter (maze on the left). No-exit mazes were those in which the main path led to a blind ending (maze on the right).

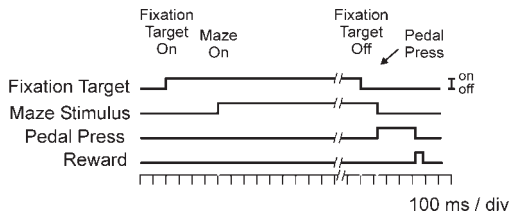


Figure 2. Sequence of events in the maze task. Each trial began when the monkey fixated the fixation target. After a variable fixation period of 600–840 ms, a maze stimulus appeared surrounding the fixation target. The maze remained visible throughout a variable delay period of 2000–2500 ms, after which the fixation target dimmed, signaling the monkey to respond. The monkey indicated whether the maze was an exit or a no-exit maze by pressing one of two foot pedals. The monkey was required to depress the response pedal for 300 ms. If the monkey correctly identified the exit status of the current maze, it received a drop of juice reinforcement. If the monkey pressed the wrong pedal, a brief pulse of white noise was presented on a small speaker.

a 2–2.5 s variable delay, the fixation target dimmed (go signal), and the monkeys indicated whether or not the path exited the maze by pressing one of two pedals with their left or right foot. The monkey held the pedal for 300 ms, after which it was given a juice reward for a correct trial or white noise was sounded for an incorrect trial. If the monkey's eye position deviated 1.5 DVA or more from the fixation target from the time of initial fixation to reward, the trial was aborted. A timeline of the task is shown in Figure 2. For each set of cells recorded, monkeys performed 160 correct trials. These 160 trials were equally divided between exit and no-exit mazes (80 trials of each type), and also between the eight possible path directions (20 trials of each direction, half exit, half no-exit). The ten repetitions of each combination of path direction and exit status were composed of two repetitions of five unique, randomly generated mazes each. A new set of mazes was randomly generated before each day of neural recording.

The monkeys also performed three control tasks: a delayed saccade task, an automated receptive field mapping task, and a grid task. In the delayed saccade task, they fixated a central spot for 500–750 ms, after which a peripheral target appeared in one of eight radial locations at an eccentricity of 15 DVA (the radius of the maze). After a variable delay of 800–1000 ms, the fixation spot disappeared and the monkeys made a saccade to the target and held fixation there for 500–750 ms to receive a reward. In the receptive field mapping task, the monkeys maintained fixation on a central spot while a mapping stimulus sequentially appeared for 130 ms in various locations. The mapping stimulus was an unfilled square equal in each dimension to the width of the maze path

(2.7 DVA). The line segments comprising the sides of the square were identical in width (0.16 DVA), luminance, and color (white) to the lines comprising the maze. The interstimulus interval between successive mapping stimuli was 325 ms. After a sequence of four to seven stimuli was shown, the fixation spot changed from blue to either red or yellow. The monkey pressed the right or left pedal, respectively, to receive a juice reward. The mapping stimuli were presented at random locations within the same region of the visual field previously occupied by the maze. During neural recordings of all tasks, the monkeys' arms were lightly restrained.

Finally, we showed maze stimuli to a monkey that was not trained to solve mazes (monkey τ). In this experiment, maze stimuli were presented for a variable period of 1–1.5 s, after which the maze stimulus dimmed slightly. If the monkey responded to the dimming with a press of a left foot pedal within 600 ms, it was rewarded. Ocular fixation at the central spot was enforced throughout the entire trial.

Neural and behavioral data acquisition

The electrical signals of neural impulse activity of single neurons were recorded extracellularly using seven (monkey κ) and 16 (monkeys π and τ) independently driven microelectrodes (Mountcastle *et al.*, 1991; Lee *et al.*, 1998) (UWE THOMAS Recording, Marburg, Germany). We recorded all cells encountered, and analyzed all cells with spontaneous activity without any preselection. Titanium recording chambers (7 mm i.d.) were placed on the skull overlying area 7a in the left cerebral hemisphere using stereotaxic information from magnetic resonance imaging (MRI) data obtained using a clinical GE 1.5 T magnet before surgery. Recording locations were verified by MRI after chamber implantation. Additionally, recording locations based on MRI were confirmed after the monkeys were sacrificed and the brains removed. All surgical procedures were done aseptically under isoflurane (2%) gas anesthesia.

Analyses

Standard statistical methods (Snedecor and Cochran, 1989) as well as more specialized analyses (e.g. bootstrap) were used to analyze the data. An analysis of covariance (ANCOVA) was performed using single trials and the following variables. The dependent variable was the average discharge rate during the delay (from maze display until the go signal), computed using fractional interspike intervals (Taira *et al.*, 1996). Path direction ($k = 8$) and exit status ($k = 2$) were fixed factors. The elapsed time since the beginning of recording of cell activity and the baseline rate during fixation before maze onset (500 ms) were used as covariates. The former covariate was used to account for time trends and the latter to account for changes in baseline firing. The level of statistical significance was set at $\alpha = 0.05$. The program 2V of the BMDP/Dynamic statistical package (BMDP Statistical Software Inc., Los Angeles, 1992) was used to execute all ANCOVAs.

With respect to the delayed saccade task, the following periods were distinguished. The visual stimulation period included the first 300 ms immediately following the onset of the peripheral stimulus; a delay/presaccadic period was defined from the end of the visual stimulation period until the onset of the saccade. Firing rates in the visual stimulation and delay/presaccadic periods of the delayed saccade task were entered as dependent variables in two separate ANCOVAs. In these analyses, target direction was the single fixed factor, and elapsed time and the firing rate during central fixation before target onset were covariates included as above.

The presence of directional tuning in neural activity during both the maze and delayed saccade tasks was assessed as follows. For cells that showed a significant main effect of direction in the relevant ANCOVA, their activity was regressed against the x - y components (i.e. direction cosines) of either the direction of the main maze path, or the saccade target direction, as described previously for the direction of movement and calculation of the preferred direction (Georgopoulos *et al.*, 1982). Analysis of spatial tuning during the maze and delayed saccade tasks was based on the task periods defined above. In a separate analysis, the activity during the first 600 ms of the delay period in the maze task was analyzed using directional statistics and a bootstrap-based significance testing (Lurito *et al.*, 1991), as follows. Each trial of neural activity was represented by a vector oriented in the direction of the corresponding maze path and scaled by the firing rate observed. These vectors were

summed across trials and path directions to yield the mean resultant. The length of the mean resultant is a measure of the strength of directional tuning. The statistical significance of the mean resultant was assessed by repeating the above procedure 30 000 times after randomly shuffling neural firing rates and path directions on a trial-by-trial basis. The proportion of the mean resultants whose length exceeded that obtained from the neural data was taken as the P value of that resultant. To determine whether the distribution of the preferred directions of the sampled cells were biased, we performed an additional bootstrap test, as follows. First, each tuned cell was assigned a unit vector in its preferred direction. The mean resultant was calculated as the vector sum of all tuned cells' unit vectors. To test the statistical significance of the length of the mean resultant, we generated the same number of unit vectors in random directions and calculated a mean resultant as above and repeated this process 30 000 times. The P value was taken as the proportion of times that the randomly generated mean resultant was longer than the actual one.

The maze population tuning curve was constructed by first standardizing individual cell tuning curves to their maximum, and then aligning them to their peaks and averaging them. Population tuning curves for the control task data were constructed by aligning the tuning functions to the direction eliciting maximal activity in the maze task for each neuron. For cells that showed a significant effect for exit status in the ANCOVA, we calculated an index of modulation of firing rate as a function of the exit status of the path. This index, M_e , was calculated by dividing the average activity for preferred exit status-mazes by average activity for non-preferred mazes. For cells the activity of which was tuned to path direction, we calculated an index of the magnitude of modulation in firing rate as a function of path direction. This index, M_d , was defined as

$$M_d = (D_{\max}/D_{\min})$$

where D_{\max} is the maximum, and D_{\min} the minimum average activity observed during the delay period, in each of the eight maze path directions.

Visual receptive fields were determined by first averaging the data from the mapping task across space (resampling from an 11×11 grid to a 5×5 grid) and then fitting a two-dimensional elliptical Gaussian function (Barlow, 1989) to the data in a nonlinear regression implemented using the IMSL statistical programming library (Visual Numerics, Houston, TX, 1995). The function fit by this regression is given by the following equation

$$f(x, y) = b + k \exp \left\{ -\frac{1}{2(1-r^2)} \left[\left(\frac{x-x_0}{s_x} \right)^2 + \left(\frac{y-y_0}{s_y} \right)^2 - 2r \left(\frac{x-x_0}{s_x} \right) \left(\frac{y-y_0}{s_y} \right) \right] \right\}$$

where (x_0, y_0) represents the center of the Gaussian, parameters b and k define the offset and depth of the tuning, respectively, and s_x and s_y define the width of tuning along two orthogonal axes. Together with parameter r , s_x and s_y also specify the angle of rotation of the ellipse and the length of the axes.

Finally, the relation between cell activity during the maze task and cell activity in the grid task was determined by calculating the circular correlation coefficient (Fisher and Lee, 1983) between the cell's preferred direction in the maze task and the direction from the fixation point to the center of its receptive field. The significance of this measure was estimated using a bootstrap test in which the directions were randomly paired (10 000 bootstrap samples).

Results

Effects of Path Direction and Exit Status on Neural Activity

We analyzed the impulse activity of 1200 cells in area 7a during the delay period of the maze task (387 from monkey $\kappa\kappa$ and

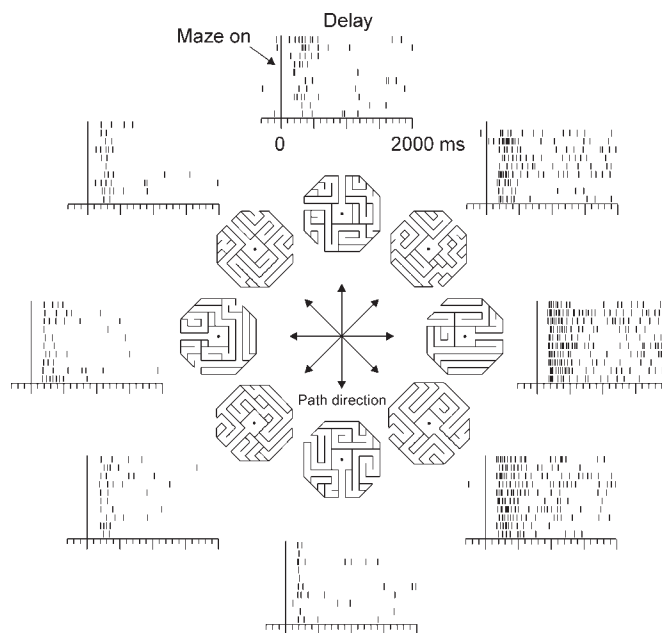


Figure 3. Rasters of impulse activity of a cell in area 7a during the maze task (monkey $\kappa\kappa$). Trials are aligned to maze onset (vertical line at 0 ms), and segregated into rasters according to the direction of the main maze path. Sample mazes with corresponding path directions are shown adjacent to each raster (mazes are spatially separated here for the purpose of illustration; each trial a single maze stimulus appeared centered in the display surrounding the fixation target).

813 from monkey $\pi\pi$). Both monkeys performed the maze task at a high level of percent correct performance (89% in monkey $\kappa\kappa$, and 98% in monkey $\pi\pi$). Generally, activity of area 7a neurons increased shortly after maze onset, and was modulated by the two main maze parameters of path direction and exit status. An example of these effects on the activity of single neurons in area 7a is shown in Figures 3–5. In the cells illustrated in Figures 3 and 4, the frequency of neural discharge was tightly aligned to maze onset, and varied systematically as a function of the radial direction of maze path. Mazes in which the path was directed to the right elicited the maximal activity from the neuron in Figure 3. Flanking path directions evoked less activity. Maximal activity was elicited in the neuron illustrated in Figure 4 when the maze path was oriented to the upper right. The exit status of the path could also influence neural activity, although this was typically a smaller effect than direction. Figure 5a shows histograms of the activity of the neuron illustrated in Figure 3 collapsed across directions, but segregated according to path exit status. Exit mazes evoked greater activity evident as a slightly higher firing rate during the delay period ($P < 0.001$, ANCOVA, see below). Figure 5b shows similar histograms of the activity of the cell illustrated in Figure 4. In this case, exit status did not affect firing rate ($P > 0.7$, ANCOVA).

The statistical significance of the effects of path direction and exit status on neural activity was assessed in an ANCOVA. We found that 529/1200 (44%) cells in the two monkeys showed a significant main effect of direction. Of all cells recorded without preselection in area 7a, the direction of the path in the maze significantly influenced the activity of nearly 1 out of every 2 cells. In addition, 262/1200 (22%) of the neurons in area 7a showed a significant main effect of exit

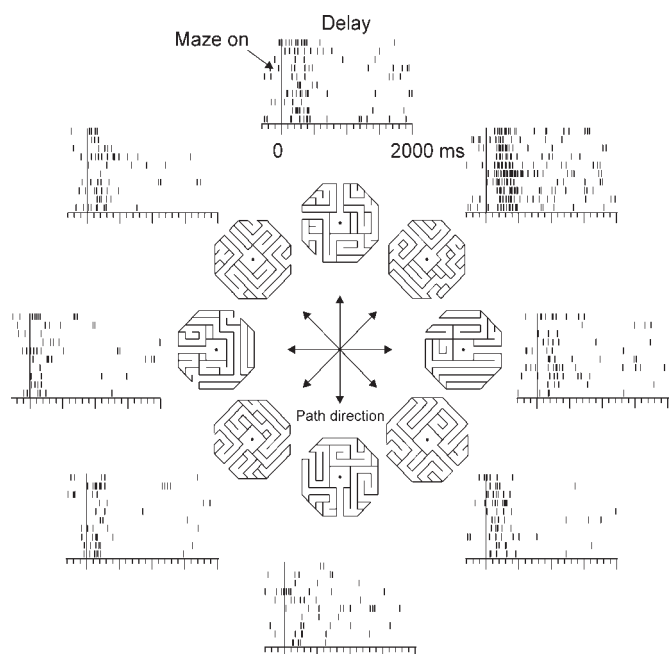


Figure 4. Rasters of impulse activity of another cell in area 7a during the maze task (monkey $\pi\pi$). Conventions are as in Figure 3.

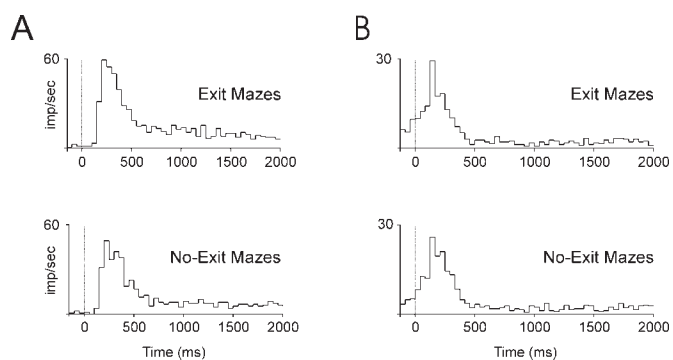


Figure 5. Comparison of activity on exit and no-exit mazes. Histograms illustrate the activity of the same neurons in Figures 4 and 5 (in panels A and B of this figure respectively), on exit and no-exit mazes, collapsed across the direction of the main maze path. Time 0 is maze onset.

status. We calculated a measure of the strength of the exit status effect, M_e , which was obtained by dividing a cell's activity on mazes with the preferred exit status by activity on non-preferred mazes. The median value of M_e across all cells significant for exit status was 1.6. Finally, 345/1200 (29%) showed a significant direction-by-exit interaction. These results are summarized in Table 1.

Spatial Tuning of Neural Activity to Maze Path Direction

To further analyze the directional properties of the neural signal observed in area 7a, we performed a directional tuning analysis to quantify the variation of firing rate as a function of path direction. First, we performed a linear regression analysis on the activity of cells that showed a significant main effect for direction in the above ANCOVA. In this analysis, the average firing rate in the delay period was regressed onto the sine and

Table 1

Factors	Significant cells (%)	
	$\kappa\kappa$ and $\pi\pi$	$\tau\tau$ (naïve)
Direction	44 (529/1200)	15 (43/279)
Exit	22 (262/1200)	5 (13/279)
Direction \times Exit	29 (345/1200)	6 (17/279)
Tuned	23 (280/1200)	1 (4/279)

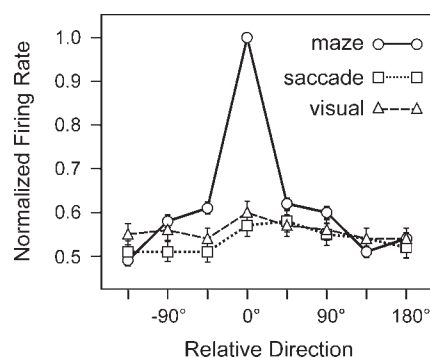


Figure 6. Population tuning in area 7a for maze path and saccade target direction. Solid line; population tuning in the delay period of the maze task. The tuning function of each cell is realigned to the path direction eliciting the maximal activity (indicated by 0°), normalized to the peak of the function, and then averaged across the population. Dashed line; population tuning in the visual stimulation period of the delayed saccade task. Dotted line; population tuning in the delay and presaccadic period of the delayed saccade task. The tuning function of each cell on the control tasks is realigned to the preferred path direction of the same cell in the maze task. Symbols are means \pm 2 SEM.

cosine of path direction. Of the 529 area 7a cells that showed an effect of direction, 280 (53%) were significantly cosine-tuned. Thus the activity of 23% (280/1200) of all cells encountered varied regularly with path direction. To confirm this result, we employed a different analytical technique. This procedure used the mean resultant calculated from the average activity in each of the eight path directions, coupled with a bootstrap procedure for significance testing. This analysis does not assume any specific tuning model. The results of this analysis were nearly identical to the results of the regression analysis above (nearly all of the neurons significantly tuned in one analysis were significantly tuned in the other). The average population tuning curves are shown in Figure 6. The population response was restricted largely to a single preferred path direction. The preferred path directions of individual cells were distributed throughout all 360° (Fig. 7) but they were significantly skewed to the right (i.e. the contralateral visual hemifield; $P < 0.001$, bootstrap test, see Materials and Methods). The mean resultant of this distribution was directed at 17° , and is indicated by the direction of the arrow in Figure 7.

We examined the possibility that the variation in neuronal response to each maze was a function of the predominant orientation of the line segments within it, and not of the direction of the path. In an analysis of the visual maze stimuli, we found that the direction of the path had an influence on the orientation of line segments comprising the maze. In the case

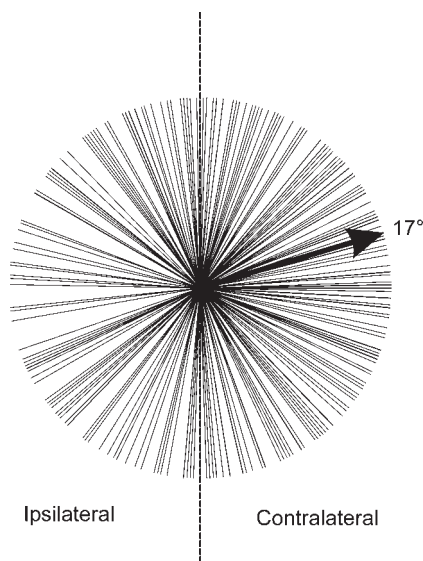


Figure 7. Distributions of preferred path directions in the maze task. Each tuned cell is represented by a line pointing in its preferred direction. Neural recordings were in the left hemisphere, lines directed to the right represent contralateral path directions. Preferred directions are distributed to both ipsilateral and contralateral hemifields, but are skewed toward the later — the mean resultant pointed to 17° (arrow).

of mazes with horizontal paths, for example, there were slightly more horizontal line segments (54%) than vertical line segments (46%) in the stimulus. Equivalent proportions of line segments parallel and orthogonal to the main path were evident in other path orientations. A possible account for the basis of the directional signal which was observed during maze solution is that neurons in area 7a are responsive to the orientation of the line segments that comprise the maze, and that this slight difference in orientation is effective in driving the cells. Because there was no significant difference in the proportions of parallel and orthogonal line segments between pairs of mazes with oppositely oriented paths (*t*-test, $P > 0.1$), a population of neurons responding to the orientation of line segments would be expected to exhibit a bimodal tuning function (responding equivalently to mazes with oppositely oriented paths). However, population tuning functions were unimodal in significantly tuned neurons (Fig. 6). Similarly, in the population of neurons that were not tuned but were significantly influenced by path direction (in the ANCOVA), neurons did not exhibit comparable neural responses to oppositely oriented paths. A 2-fold difference was evident in the response of this population to preferred and opposite path directions. These data strongly favor the conclusion that the directional signal observed in parietal cortex during maze solution reflects the direction of the path, and not the predominant orientation of line segments at other points within the maze stimulus.

In order to quantify the depth of the modulation of activity with path direction for each neuron, we calculated the ratio between the average delay period activity when mazes with most and least preferred path directions were shown (M_d , Materials and Methods). The median value of M_d was 3.04. Eleven cells had an infinite magnitude index because the minimum was 0. When these cells were left out of the analysis, the mean value of the index was 4.56. Figure 8 shows the frequency distribution histogram of the magnitude M_d . The size of this index indicates that, on average, tuned neurons in area

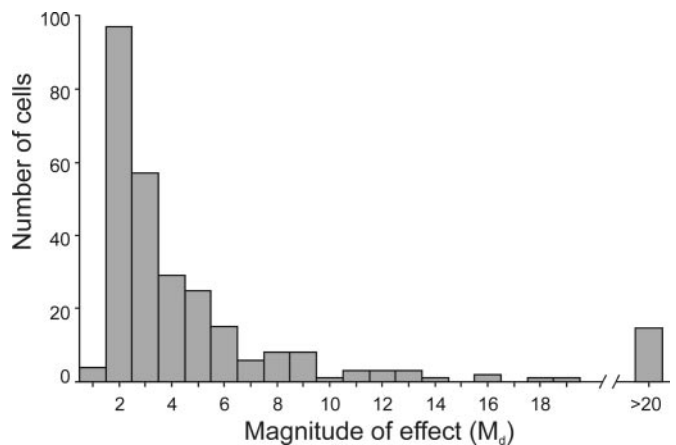


Figure 8. Frequency distribution histogram of the response magnitude index, M . M is defined as D_{\max}/D_{\min} , where D_{\max} is the maximum average delay period activity observed, and D_{\min} the minimum average delay period activity observed, in each of the eight maze path directions.

7a exhibited at least a 4-fold change in firing rate as a function of path direction. The depth of modulation in Figure 6 is less than the average magnitude, M_d , because rate minima in individual tuning functions were not aligned in the population data.

We sought to determine whether stronger responses were evident in neurons that preferred contralateral than ipsilateral path directions, by comparing the mean modulation index defined above. The mean index for the two populations of neurons that preferred ipsilateral ($M_d = 5.1$) versus contralateral (4.3) path directions did not significantly differ (Mann-Whitney test; $P > 0.1$). Finally, there was also no significant difference in the magnitude index M of directional modulation segregated by visual quadrant (Kruskal-Wallis test; $P > 0.2$).

Absence of Path Tuning in a Naïve Monkey

We also presented the same maze stimuli shown to the first two monkeys to a monkey not trained in the maze task. This animal had to maintain fixation while mazes were displayed for 1000 to 1500 ms. After this time, the maze dimmed slightly and the monkey responded with a left foot pedal press. We recorded the activity of 279 area 7a cells during the delay period of this task. We performed the same ANCOVA and tuning analyses above on the neural responses of these cells. We found that although there is some variation of firing rate with direction (43/279 or 15.4% cells significant for direction in the ANCOVA), there was no systematic tuning of these cells to path direction (4/279 or 1.4% of cells tuned). Nor were there many cells whose activity varied significantly with the path exit status (13/279, 4.7%). The results of these analyses are summarized in Table 1.

Path Tuning in the Maze Task is not Accounted for by Visual Receptive Field Position

We were interested in the degree to which directional tuning for maze path direction could be accounted for by the locations of receptive fields of area 7a visual neurons. We hypothesized that path tuning observed in the maze task might be due an interaction between the maze stimulus and visual receptive fields. Under this hypothesis, cells would exhibit spatial

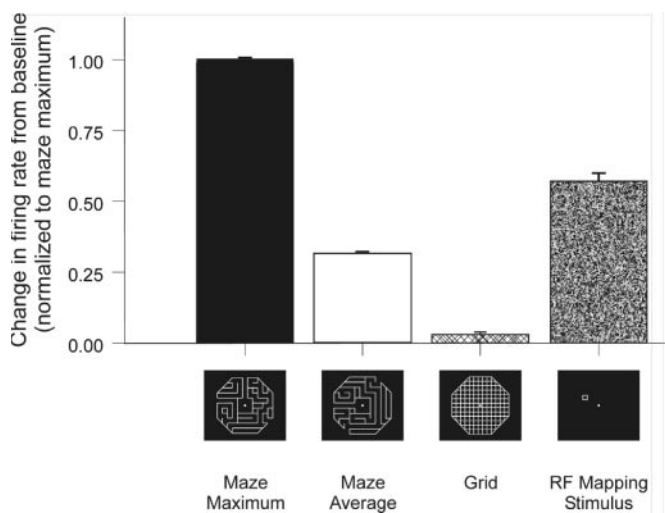


Figure 9. Magnitudes of average population responses to different classes of visual stimuli. Neural activity is expressed as a change from baseline activity, and normalized to the maze maximum. Maze maximum; mean response in the neural population to mazes of preferred path direction. Maze average; response averaged across all mazes. Grid and RF mapping stimulus, mean population response to the grid and mapping stimuli.

tuning to path direction if the main maze path in particular orientations would traverse their visual receptive fields. To test for this possibility, we mapped visual receptive fields using an automated procedure (see Materials and Methods). The majority of the maze path tuned neurons were visually responsive when tested with the visual mapping stimulus. Of the cells tuned in the maze task and recorded on the receptive field mapping task, 66% (83/126) showed an average activation two standard deviations above baseline for at least 10% of stimulus locations. The average response of tuned cells to the mapping stimulus, relative to activity on the maze task, is shown in Figure 9 (rightmost bar). It can be seen that the response to the mapping stimuli was higher than that of the average of the mazes (second bar from left), but less than the activity of preferred mazes (leftmost bar).

We modeled receptive fields by fitting two-dimensional Gaussian surfaces to the firing rates evoked by the mapping stimulus at different locations. The activity of many cells that were tuned in the maze task was fit well by this model. For example, 53% of cells were fit by a model with an R^2 above 0.2, and 21% of cells had an R^2 of 0.5 or higher. Because it is difficult to assign an accurate significance level to these results (a nonlinear regression was used to fit the data), we performed the analyses below multiple times, on five overlapping groups of cells. These groups were composed of all cells with a regression fit above five levels: $R^2 \geq 0.2, 0.3, 0.4, 0.5,$ and 0.6 . This analysis allowed for a direct comparison between the direction from the fixation point to the center of receptive fields defined by this procedure, and the preferred path directions of the same neurons measured in the maze task. We found little systematic relationship between tuning in the maze task and the locations of receptive fields, at any of the R^2 levels defined above. Specifically, there was no correlation between the direction to the center of cells' receptive fields and the direction of the maze path for which a cell responded the most. The range of circular correlation coefficients observed was $\hat{\rho}_t = -0.002$ to 0.008 , $P \approx 0.56$ to 0.17 , bootstrap test (see Materials and Methods). The highest level of significance was found for

the $R^2 \geq 0.2$ group. We also found a large range of angular distances between the preferred maze direction and the center of the cells' receptive fields. For all groups studied, we found that no higher than 21.4% of cells had an angular difference $<45^\circ$ (range 13.9% for the $R^2 \geq 0.6$ group to 21.4% for the $R^2 \geq 0.4$ group). The four panels of Figure 10 compare the locations of the visual receptive fields and the preferred maze path directions of four area 7a neurons. Each maze depicts the path direction preferred by a single neuron superimposed on a map of that cell's visual receptive field. The preferred path direction was aligned with the center of the visual receptive field in some neurons (lower left, for example), however in the majority of cells, the preferred path and visual receptive field were not aligned. A distribution of the angular differences between the preferred path direction and the centers of receptive fields is shown in Figure 11.

We performed an additional analysis that did not depend on a Gaussian model of receptive field structure. For this purpose, we calculated the average firing rates evoked by the mapping stimulus presented within eight rectangular regions of space. Each region overlapped the main path in one of its eight directions, and was as long as the main path and three times as wide. This yielded eight average firing rates per cell, which were then correlated with the cell's average activity observed for the eight corresponding directions of the main path during the maze task. Across the population of cells significant for direction in the maze task and recorded in the mapping task, there was no systematic correlation between these two measures. Only 6.4% of cells in the sample were significantly correlated ($P < 0.05$). Additionally, we tested the possibility that tuning to maze path direction reflected variations in visual responsiveness in the perifoveal regions of space where the gap in the start box appeared. The location of this gap, representing the origin of the maze path, correlated with path direction, and stimulation of visual receptive fields by this feature of the start box may have accounted for path tuning. We tested for this possibility by correlating the firing rates of individual neurons observed during the maze and RF mapping tasks, selecting those RF stimulus locations overlapping the region occupied by the gap in the start box. This circular correlation was significant at a $P < 0.05$ level in only 1.6% of the sample of neurons tested, a number not greater than the proportion expected by a chance relation given the alpha level of the test.

In another visual task, the monkeys were shown an octagonal grid stimulus, the same size and spatial frequency as the maze (Figure 9, 'grid'). The grid stimulus was equivalent to maze stimuli with all possible line segments present. The grid was shown for 2000–2500 ms, after which the fixation spot changed color, and the monkeys responded by pressing one foot pedal or the other, depending on the new color of the fixation spot. We found that only 10% (24/234) of cells significant for direction in the maze task were significantly activated by the grid stimulus (t -test) and that 16/135 (12%) of cells tuned in the maze task were activated by the grid. The grid was in general an ineffective stimulus (Figure 9, 'Grid').

Path Tuning in the Maze Task is not Accounted for by Oculomotor Planning

To test for the possibility that activation on the maze task could be due to saccade planning, we trained monkeys to make delayed saccades to eight circular targets presented at an eccentricity equal to the radius of the maze, and in the direc-

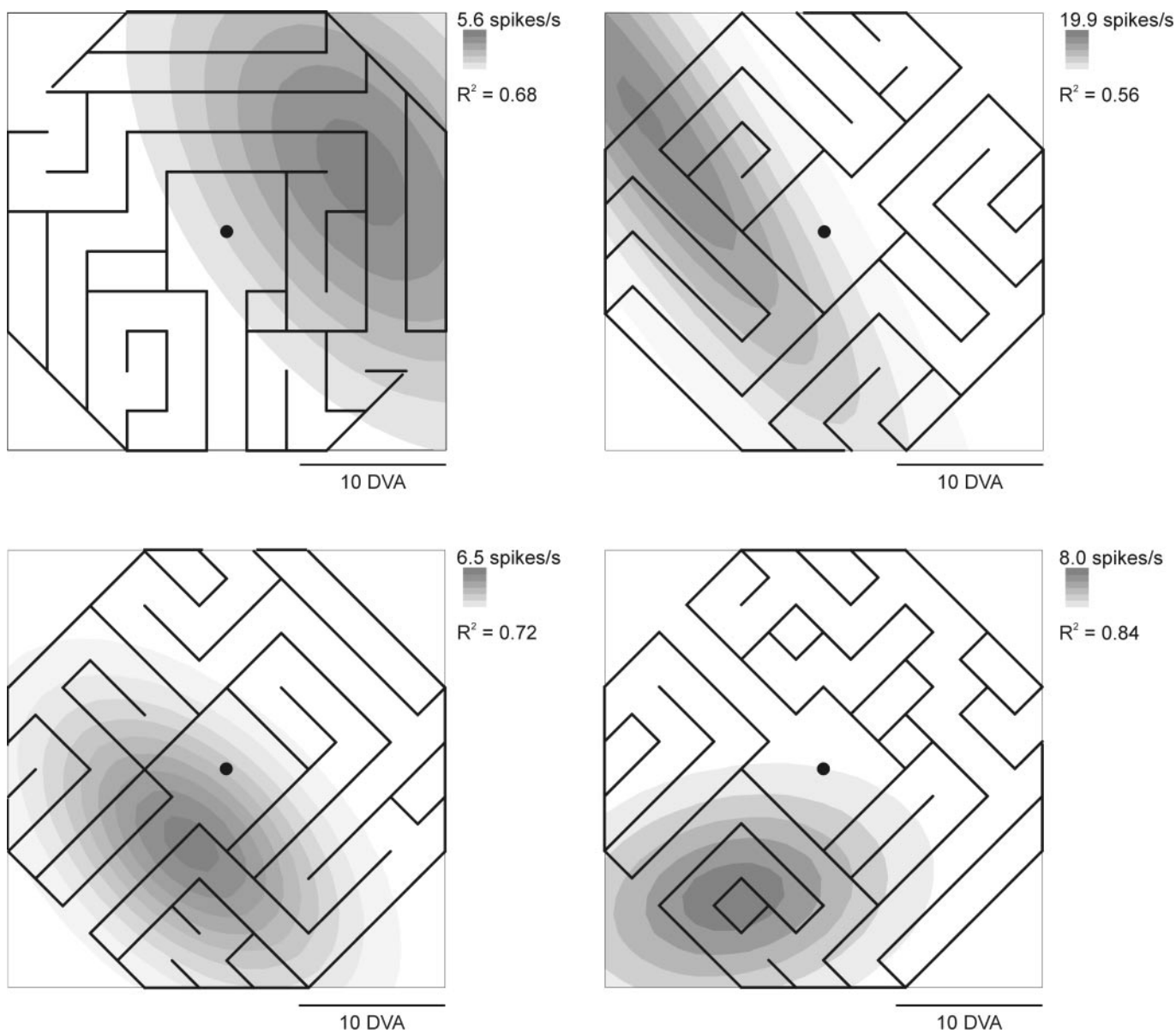


Figure 10. Comparison of visual receptive field location and preferred path orientation. The location and shape of the visual receptive fields of four area 7a neurons are shown as contour plots in each panel. The preferred maze path orientation of each neuron is indicated by the path orientation in the superimposed example maze. The quality of the fit between the Gaussian surface and neural firing elicited by the mapping stimulus is indicated by the r^2 value adjacent to each plot. DVA, degrees visual angle.

tions of the eight radial maze paths. We found that in the large majority of cells, spatial tuning for path direction in the maze task was not systematically related to spatial tuning for saccade direction in the oculomotor control task. Populations of neurons whose activity was significantly influenced (ANCOVA) by path or target direction in the two tasks (and recorded in both) are represented by the blue (maze task) and yellow (saccade task) circles in Figure 12. As can be seen in this figure, these subpopulations were only partially overlapping. Of the 236 neurons whose activity was influenced by path direction in the maze task, only 28% were influenced by saccade direction in the oculomotor control task (intersection between blue and yellow circles, Fig. 12a). Few (30%) of the cells active during maze solution were significantly active during the oculomotor control irrespective of directional effects. In addition,

neural firing rates across maze path direction and saccade target direction were uncorrelated in most of these cells (208/236, 88%), at a liberal probability level ($P > 0.1$). Additionally, only 15% (35/236) of these neurons had the same preferred directions in the two tasks. This percentage did not differ significantly from the chance level of 20% (test of binomial proportions: given five possible intervals between eight directions in the unit circle arranged every 45° , the expected proportion by chance for any interval is $1/5 = 20\%$). Finally, when the analysis was restricted to 142 neurons that were tuned in the maze task, we found that 74% (105/142) of these cells were not significantly tuned in the delay/presaccadic period of the oculomotor task. In the remaining 37 neurons that were tuned in both tasks, we found that the maxima of the spatial tuning functions were not systematically aligned. One

half of these cells (18/37) had preferred directions greater than 60° apart. Figure 12b shows the range of differences in preferred directions in the maze task and the delay/presaccadic period of the oculomotor task for these 37 cells. The radial lines bounding each sector represent the preferred directions

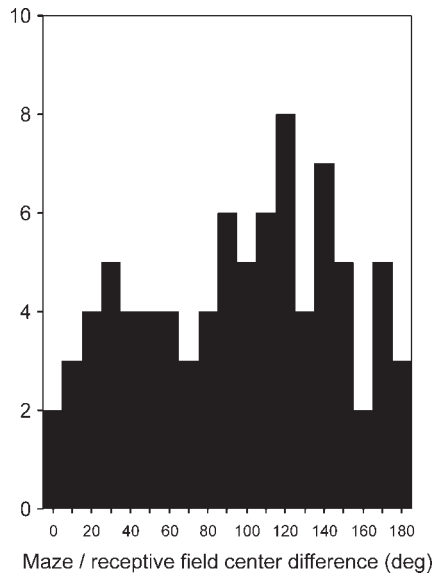


Figure 11. Distribution of angular differences between preferred path direction in the maze task and receptive field locations in the RF mapping task. For comparison to the preferred path direction, receptive field location is represented as a direction from the fovea to the RF center. Data shown are for receptive fields fit at $r^2 \geq 0.4$. This group showed the greatest alignment between preferred path direction and RF location.

in the two tasks for each cell. Overall <10% of neurons were tuned in both tasks and had preferred directions that were within 20° of each other. In fact, the normalized, averaged population tuning function of the 142 neurons above, aligned to the preferred maze path direction, did not exhibit a peak in the same direction during the saccade period of the oculomotor task (dotted line, square symbols, Fig. 6). We also performed the above analyses excluding the delay period using a more constrained perisaccadic window spanning movement initiation (-100, +50 ms relative to saccade onset) and found similar results, but with even less congruency between the maze and saccade cells. For example, 15% of cells tuned in the maze task were also tuned in the perisaccadic period of the oculomotor task, versus 28% for the delay/presaccadic window.

Finally, we compared neural activity in the maze task to the activity of the same neurons in the visual period of the delayed saccade task. We used the same set of analyses that were applied to activity in the delay/presaccadic period of this task, as above. Nearly identical results were obtained. For example, most (79%) cells were not significantly activated during this period, and most (81%) of the cells that were influenced by path direction in the maze task were not influenced by the location of the visual stimulus in the delayed saccade control task. Of those that were active and directionally tuned in both tasks, preferred directions were not systematically related (Fig. 6, triangles).

Locations of Recorded Neurons

Recording locations in area 7a were determined by magnetic resonance imaging (MRI). MRI images were used to recon-

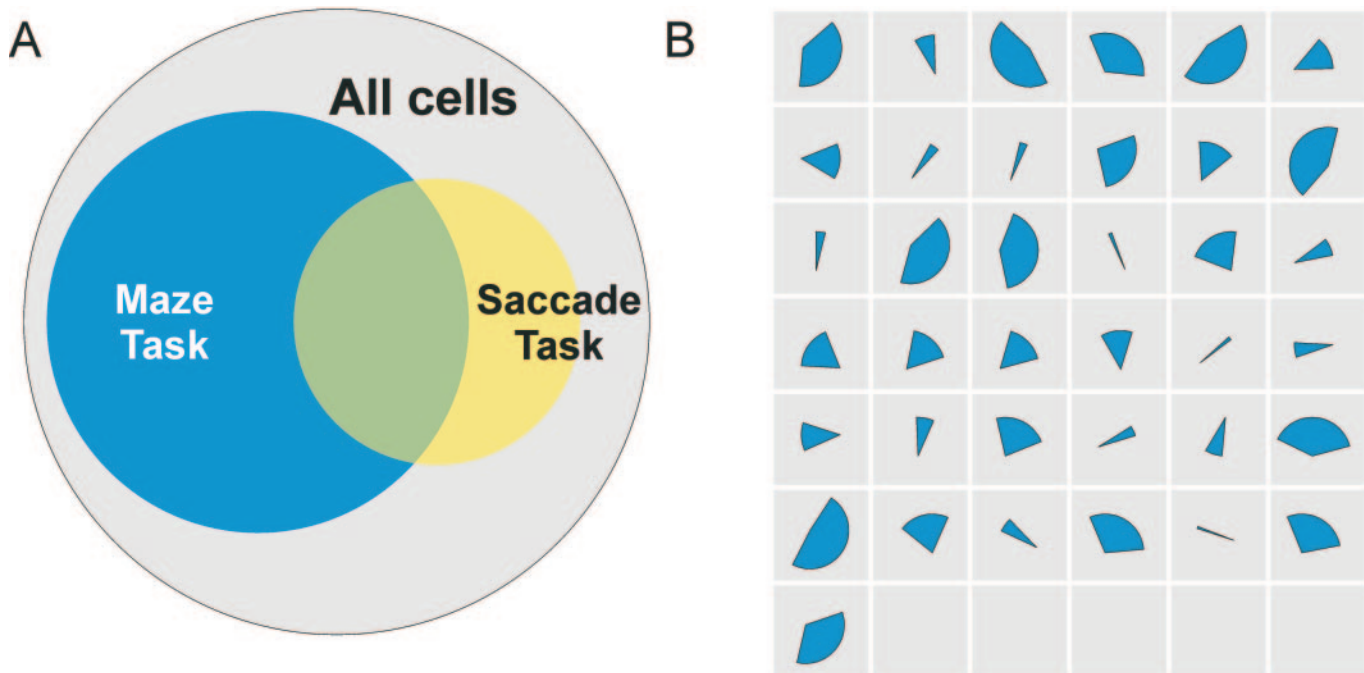


Figure 12. (A) Venn diagram displaying the percentage of all cells significant for direction during the maze task (blue circle), the delay and presaccadic period of the delayed saccade task (yellow circle), and during both tasks (blue/yellow intersection). The populations indicated represent the subset of neurons recorded in both tasks. (B) Comparison of the preferred directions on maze and saccade tasks of the 37 cells that were significantly tuned in both. The radial lines bounding each sector represent the preferred directions of a single cell during the delay period of the maze task and the delay and presaccadic period of the delayed saccade task.

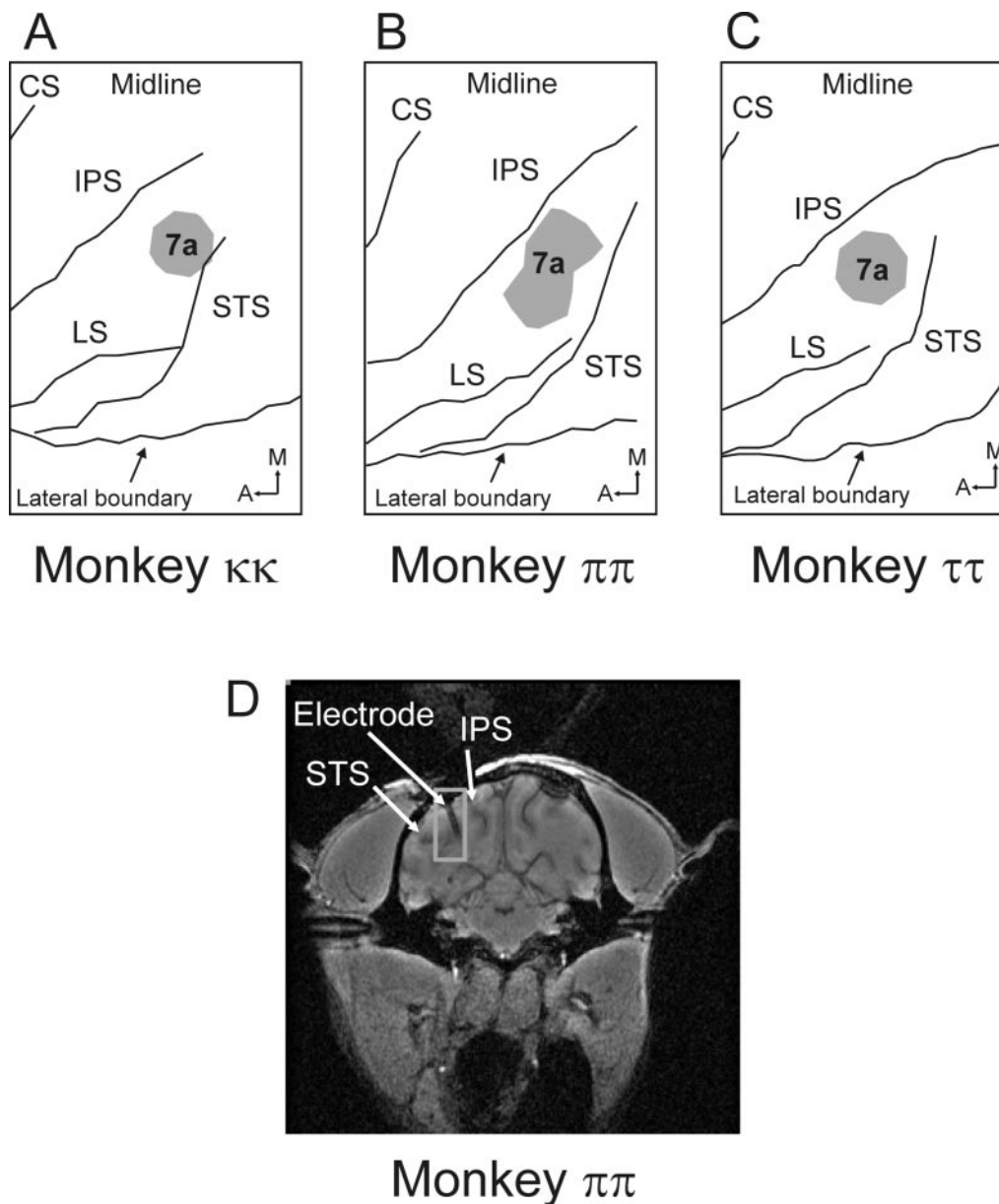


Figure 13. (A–C) Region of area 7a recordings as reconstructed from MRI images for the three monkeys; the gray regions indicate the recording locations. Monkeys $\kappa\kappa$ and $\pi\pi$ were trained in the maze task, monkey $\tau\tau$ viewed mazes but was not required to solve them. (D) MRI image of an electrode inserted through the center of the recording chamber of monkey $\pi\pi$. CS, central sulcus; IPS, intraparietal sulcus; LS, lateral sulcus; STS, superior temporal sulcus; M, medial; A, anterior.

struct the sulcal pattern of the cerebral cortex, and recording penetrations were superimposed on this reconstruction (Fig. 13a–c). In one animal, the recording location determined in this manner was confirmed by localizing the position of an electrode centered in the recording chamber in the brain with MRI. The electrode can be seen in MRI images to enter area 7a between the superior temporal and lateral sulci (Figure 13d). Finally, the locations of recording sites derived from MRI images were confirmed in the fixed brains after sacrifice.

Discussion

Area 7a is known to function in spatial processing as this relates to sensorimotor integration and visual attention. This study addressed the question whether this region of parietal cortex might also contain neural signals that relate to spatial

cognition, specifically, a goal driven, analytical process applied to the visual input. To address this question, we compared the activity of single neurons in area 7a of monkeys performing a visual maze task with the activity of the same neurons on traditional sensorimotor paradigms. In the visual maze task, monkeys viewed a maze stimulus, and indicated whether a single path reached an exit at a gap in the maze perimeter or a blind ending within the maze instead. The solution to the problem posed by the task required that subjects determine the ending of the critical path, which in turn required prior determination of its continuity with the start box.

Prior studies of maze solution in both human and nonhuman primate subjects suggested that the continuity of the critical path, and its course through the maze, was determined by a spatial analysis under way while the position of the eyes

remained fixed (Crowe *et al.*, 2000; Chafee *et al.*, 2002). The time taken to analyze a section of maze path depended on its length and the number of turns it contained. This was evident during periods of fixation interspersed between saccades when eye movements were allowed (Crowe *et al.*, 2000), or in the time taken to solve mazes when eye movements were prohibited (Chafee *et al.*, 2002). In order to locate and identify the end of the critical path, the spatial analysis inferred from the above data may be required to encode the direction of that path, as this direction in turn defines the part of the maze where the exit to the critical path is located. The present study revealed that the activity of nearly one in four 7a neurons was systematically tuned for the direction of the critical path.

Path Tuning Is Associated with Maze Solution not Maze Viewing

We considered the effect of maze path direction on neural activity in area 7a of three monkeys. Two of them determined the exit status of the maze, one detected a dimming of the same stimulus. There was a clear difference in the incidence and type of directional activity encountered in area 7a of monkeys solving mazes versus the monkey that was simply viewing mazes. During maze solution, about one-quarter (23%) of all the neurons we encountered in area 7a of the trained animals was significantly tuned with respect to maze path direction. During maze viewing, only 1% of neurons in area 7a of the naïve animal were tuned to path direction. Therefore, the cognitive requirement of maze solution influenced neural activity in parietal cortex. This influence appeared to be distinct from the properties of the visual stimulus.

Maze Path Tuning and Visual Receptive Fields in Area 7a

Visual receptive field mapping was intended to serve as a probe for a possible mechanism for maze path tuning. Our initial hypothesis was that path tuning observed in the maze task might be due an interaction between the maze stimulus and visual receptive fields. In this case, visually responsive neurons in parietal cortex would be preferentially activated when the processed path traversed their receptive field. Visual receptive fields in area 7a are large and peripheral (Motter and Mountcastle, 1981), and many area 7a neurons are driven by simple, stationary, stimuli such as spots or squares of light (Motter and Mountcastle, 1981; Andersen and Mountcastle, 1983; Steinmetz and Constantinidis, 1995; Chafee and Goldman-Rakic, 1998; Snyder *et al.*, 1998; Bender and Youakim, 2001; Constantinidis and Steinmetz, 2001).

The majority of neurons that were tuned to path direction during maze solution were visually responsive – the receptive field mapping stimuli activated two-thirds of the sample.

Under the above hypothesis, visual receptive fields would prove to be on or near the preferred maze path. The evidence did not support this hypothesis. We found that visual receptive fields and preferred maze paths were not systematically aligned. This spatial independence was documented by two analyses, one of which depended on a Gaussian model of visual receptive fields, and another in which we correlated firing rates on maze and visual control tasks directly. Additional evidence was provided by the dissociation of spatial tuning in the maze task and that seen in response to the visual stimulus serving as a saccade target in the oculomotor control task.

Because the receptive field mapping stimuli were considerably different from the maze stimulus, some caution is warranted before concluding that activity during maze solution is entirely independent of visual receptive field mechanisms. If a visual receptive field mechanism accounts for path tuning in the maze task, this mechanism should then be context dependent. We cannot rule out this possibility. Visual receptive field properties in area 7a neurons vary as a function of the attributes of the mapping stimulus used (Motter *et al.*, 1987; Merchant *et al.*, 2001). It has also been shown that behavioral context influences visual receptive field structure in parietal area LIP (Ben Hamed *et al.*, 2002), and that receptive fields in this cortical area can shift before saccades (Duhamel *et al.*, 1992).

Maze Path Tuning and Oculomotor Intention in Area 7a

The directional signal encoded by path tuned neurons did not appear to be related to movement planning, since it was observed while monkeys maintained ocular fixation of a stationary target at the center of the maze. The parameter of path direction encoded by neural activity was not associated with the direction of the motor response required by the task. As parietal cortex has been associated with motor intention (Andersen *et al.*, 1997; Andersen and Buneo, 2002), we examined the possibility that path tuning might reflect a form of motor planning. In this view, it can be argued that maze path tuning in area 7a neurons reflects the monkey's intention to make a saccade (which is never executed or rewarded) whose direction is linked to the orientation of the critical path in the maze. Neural activity in area 7a would in this case reflect an oculomotor plan and not path processing. Several lines of evidence argue that area 7a has a minor role in saccade execution and control, particularly in comparison to area LIP. Microstimulation that evokes saccadic eye movements in area LIP does not evoke eye movements in area 7a (Thier and Andersen, 1998). The anatomical connections of area 7a to other oculomotor centers such as the frontal eye fields are weak in comparison to the projections linking LIP and the FEF (Andersen *et al.*, 1990). Finally neurons in area 7a are active mostly following saccadic eye movements (Barash *et al.*, 1991), and so are not likely to play as prominent a role in initiating them. However, area 7a is reciprocally connected with area LIP (Cavada and Goldman-Rakic, 1989; Andersen *et al.*, 1990; Baizer *et al.*, 1991), 7a neurons are activated at the time of saccadic eye movements (Barash *et al.*, 1991; Chafee and Goldman-Rakic, 1998), and are also tuned for saccade direction (Chafee and Goldman-Rakic, 1998). Consequently, the argument that neural activity in this cortical area reflects motor intention cannot be ruled out entirely. To address this alternative interpretation of path tuning, we recorded the activity of a subset of neurons influenced by path direction during maze solution (as assessed by the ANCOVA) on a delayed saccade control task. We found that of those cells tuned to path direction during maze solution, most were inactive on the oculomotor control task. Furthermore, fewer cells were tuned to target location while monkeys planned saccades. Considering the small minority of cells that were tuned in both tasks, we found that the preferred directions were not necessarily aligned (Fig. 12). These results argue against the possibility that path tuning seen during maze solution is simply due to oculomotor intention.

Parietal Cortex and Spatial Attention

Attention modulates visual responsiveness in area 7a. Mountcastle and co-workers (Mountcastle *et al.*, 1981; Mountcastle *et al.*, 1987) found that responses of 7a neurons to peripheral visual stimuli were enhanced when the monkey was attentively fixating, in comparison to identical stimuli presented during inattentive eye pauses. Steinmetz and Constantinidis (Steinmetz and Constantinidis, 1995) found that stimuli delivered at attended locations evoked diminished neural responses in area 7a compared to stimuli presented at unattended locations. Robinson and colleagues (Robinson *et al.*, 1995) similarly found that neural responses in area 7a to stimuli at unattended locations were larger than when the same stimuli were delivered at the current locus of attention. Neurons in area 7a respond preferentially to salient stimuli in multistimulus displays (Gottlieb *et al.*, 1998; Constantinidis and Steinmetz, 2001). Because neural activity is greatest when the locus of visual stimulation and visual attention are disjoint, the theory has been put forward that neural activity in area 7a serves to shift the locus of attention (Steinmetz and Constantinidis, 1995). A recent study of area LIP provides compelling evidence that the spatial coordinate encoded by neural activity in this parietal area was linked to the current locus of covert visual attention (Bisley and Goldberg, 2003). Activation of human parietal cortex in tasks requiring covert shifts of visual attention in the absence of overt movement has been a common finding (Corbetta *et al.*, 1993, 1995; Nobre *et al.*, 1997; Coull and Nobre, 1998). Neural activity in area 7a during maze solution may be related to shifts of visual attention that occur along the path direction in order to determine the exit status of the path. However, the location of visual attention during maze solution was not explicitly measured.

Area 7a Participates in Both Maze and Sensorimotor Processing

In area 7a we found a population of neurons that was involved in maze processing, a population of neurons that was responsive to spot visual stimuli, and a population that was active in relation to saccadic eye movements. The primary result was that these were for the most part distinct populations. In the minority of 7a neurons activated during maze solution and during the sensorimotor control tasks, the spatial tuning functions of individual neurons were not systematically aligned in the two conditions. The implication is that individual neurons can participate in diverse neural representations of space, and that to a degree, these representations may be independent even in single neurons. The neural representation of space in area 7a that we have observed requires both the maze stimulus, and the cognitive requirement of solving mazes. Path tuning did not occur in area 7a neurons when a naïve monkey viewed the same set of visual maze stimuli. We suggest that the neural representation of path direction in area 7a reflects a specific form of spatial cognition recruited by maze solution.

Notes

Supported by USPHS grant NS17413, the United States Department of Veterans Affairs, and the American Legion Brain Sciences Chair.

Address correspondence to Apostolos P. Georgopoulos, Brain Sciences Center (11B), Veterans Affairs Medical Center, One Veterans Drive, Minneapolis, MN 55417, USA. Email: omega@umn.edu

References

- Andersen RA, Asanuma C, Essick G, Siegel RM (1990) Corticocortical connections of anatomically and physiologically defined subdivisions within the inferior parietal lobule. *J Comp Neurol* 296:65–113.
- Andersen RA, Buneo CA (2002) Intentional maps in posterior parietal cortex. *Annu Rev Neurosci* 25:189–220.
- Andersen RA, Mountcastle VB (1983) The influence of the angle of gaze upon the excitability of the light-sensitive neurons of the posterior parietal cortex. *J Neurosci* 3:532–348.
- Andersen RA, Snyder LH, Bradley DC, Xing J (1997) Multimodal representation of space in the posterior parietal cortex and its use in planning movements. *Annu Rev Neurosci* 20:303–330.
- Baizer JS, Ungerleider LG, Desimone R (1991) Organization of visual inputs to the inferior temporal and posterior parietal cortex in macaques. *J Neurosci* 11:168–90.
- Barash S, Bracewell RM, Fogassi L, Gnadt JW, Andersen RA (1991) Saccade-related activity in the lateral intraparietal area. I., Temporal properties; comparison with area 7a. *J Neurophysiol* 66:1095–1108.
- Barlow R (1989) *Statistics*. New York: Wiley.
- Ben Hamed S, Duhamel JR, Bremmer F, Graf W (2002) Visual receptive field modulation in the lateral intraparietal area during attentive fixation and free gaze. *Cereb Cortex* 12:234–245.
- Bender DB, Youakim M (2001) Effect of attentive fixation in macaque thalamus and cortex. *J Neurophysiol* 85:219–234.
- Bisley JW, Goldberg ME (2003) Neuronal activity in the lateral intraparietal area and spatial attention. *Science* 299: 81–86.
- Cavada C, Goldman-Rakic PS (1989) Posterior parietal cortex in rhesus monkey: I., Parcellation of areas based on distinctive limbic and sensory corticocortical connections. *J Comp Neurol* 287:393–421.
- Chafee MV, Averbach BB, Crowe DA, Georgopoulos AP (2002) Impact of path parameters on maze solution time. *Arch Ital Biol* 140:247–251.
- Chafee MV, Goldman-Rakic PS (1998) Matching patterns of activity in primate prefrontal area 8a and parietal area 7ip neurons during a spatial working memory task. *J Neurophysiol* 79:2919–2940.
- Constantinidis C, Steinmetz MA (2001) Neuronal responses in area 7a to multiple-stimulus displays: I., neurons encode the location of the salient stimulus. *Cereb Cortex* 11:581–591.
- Corbetta M, Miezin FM, Shulman GL, Petersen SE (1993) A PET study of visuospatial attention. *J Neurosci* 13:1202–1226.
- Corbetta M, Shulman GL, Miezin FM, Petersen SE (1995) Superior parietal cortex activation during spatial attention shifts and visual feature conjunction. *Science* 270:802–805. [Erratum: *Science* 270:1423.]
- Coull JT, Nobre AC (1998) Where and when to pay attention: the neural systems for directing attention to spatial locations and to time intervals as revealed by both PET and fMRI. *J Neurosci* 18:7426–7435.
- Crowe DA, Averbach BB, Chafee MV, Anderson JH, Georgopoulos AP (2000) Mental maze solving. *J Cogn Neurosci* 12:813–827.
- Duhamel JR, Colby CL, Goldberg ME (1992) The updating of the representation of visual space in parietal cortex by intended eye movements. *Science* 255:90–92.
- Fisher NI, Lee AJ (1983) A correlation coefficient for circular data. *Biometrika* 70:327–332.
- Fuchs AF, Robinson DA (1966) A method for measuring horizontal and vertical eye movement chronically in the monkey. *J Appl Physiol* 21:1068–1070.
- Georgopoulos AP, Kalaska JF, Caminiti R, Massey JT (1982) On the relations between the direction of two-dimensional arm movements and cell discharge in primate motor cortex. *J Neurosci* 2: 1527–1537.
- Gottlieb JP, Kusunoki M, Goldberg ME (1998) The representation of visual salience in monkey parietal cortex. *Nature* 391:481–484.
- Lee D, Port NL, Kruse W, Georgopoulos AP (1998) Neuronal population coding: multielectrode recordings in primate cerebral cortex. In: *Neuronal ensembles: strategies for recording and decoding* (Eichenbaum H and Davis J, eds). New York: Wiley.
- Lurito JT, Georgakopoulos T, Georgopoulos AP (1991) Cognitive spatial-motor processes. 7. The making of movements at an angle from a stimulus direction: studies of motor cortical activity at the single cell and population levels. *Exp Brain Res* 87:562–580.

- Merchant H, Battaglia-Mayer A, Georgopoulos AP (2001) Effects of optic flow in motor cortex and area 7a. *J Neurophysiol* 86: 1937–1954.
- Motter BC, Mountcastle VB (1981) The functional properties of the light-sensitive neurons of the posterior parietal cortex studied in waking monkeys: foveal sparing and opponent vector organization. *J Neurosci* 1: 3–26.
- Motter BC, Steinmetz MA, Duffy CJ, Mountcastle VB (1987) Functional properties of parietal visual neurons: mechanisms of directionality along a single axis. *J Neurosci* 7: 154–176.
- Mountcastle VB, Andersen RA, Motter BC (1981) The influence of attentive fixation upon the excitability of the light-sensitive neurons of the posterior parietal cortex. *J Neurosci* 1: 1218–1225.
- Mountcastle VB, Motter BC, Steinmetz MA, Sestokas AK (1987) Common and differential effects of attentive fixation on the excitability of parietal and prestriate (V4) cortical visual neurons in the macaque monkey. *J Neurosci* 7:2239–2255.
- Mountcastle VB, Reitboeck HJ, Poggio GF, Steinmetz MA (1991) Adaptation of the Reitboeck method of multiple microelectrode recording to the neocortex of the waking monkey. *J Neurosci Methods* 36:77–84.
- Nobre AC, Sebestyen GN, Gitelman DR, Mesulam MM, Frackowiak RS, Frith CD (1997) Functional localization of the system for visuospatial attention using positron emission tomography. *Brain* 120: 515–533.
- Robinson DL, Bowman EM, Kertzman C (1995) Covert orienting of attention in macaques. II. Contributions of parietal cortex. *J Neurophysiol* 74:698–712.
- Snedecor GW, Cochran, WG (1989) *Statistical methods*. Iowa State University Press: Ames IA.
- Snyder LH, Grieve KL, Brotchie P, Andersen RA (1998) Separate body- and world-referenced representations of visual space in parietal cortex. *Nature* 394:887–891.
- Steinmetz MA, Constantinidis C (1995) Neurophysiological evidence for a role of posterior parietal cortex in redirecting visual attention. *Cereb Cortex* 5:448–456.
- Taira M, Boline J, Smyrnis N, Georgopoulos AP, Ashe J (1996) On the relations between single cell activity in the motor cortex and the direction and magnitude of three-dimensional static isometric force. *Exp Brain Res* 109:367–376.
- Thier P, Andersen RA (1998) Electrical microstimulation distinguishes distinct saccade-related areas in the posterior parietal cortex. *J Neurophysiol* 80:1713–1735.